2024 IEEE/ASME International Conference on Advanced Intelligent Mechatronics (AIM)
July 15-19, 2024. Boston, MA, USA

Control Framework for Multirotors with Additional Horizontal Thrusters

Ricardo Rosales Martinez, Hannibal Paul, and Kazuhiro Shimonomura

***Abstract*— As the adoption of Unmanned Aerial Vehicles (UAVs) increases in the industrial sector, the limitations of traditional multirotors have become more noticeable. Though widely employed, conventional multirotors are under-actuated, which restricts the types and quality of manipulation task they can perform. Fully-actuated systems on the other hand, offer an interesting alternative solution with their decoupled forces. However, their widespread use is hindered by complexities in their control and design. Our proposed approach addresses this challenge by introducing multirotors equipped with horizontal thrusters, aiming to find a balance between simplicity and advanced control. These vehicles strategically incorporate additional thrust components tailored to specific tasks, thereby extending the capabilities of traditional under-actuated multirotors. We developed a control algorithm using the PX4 Autopilot to accommodate various flight modes, encompassing directional thrust flight and planar flight. To evaluate our system, we conducted simulations and tested vehicles with different actuator configurations. These simulations were then validated through real-world experiments using a UAV equipped with thrusters and a flight controller running a modified firmware with our control framework. This comprehensive approach allowed us to assess the system's performance in both simulated and practical scenarios.**

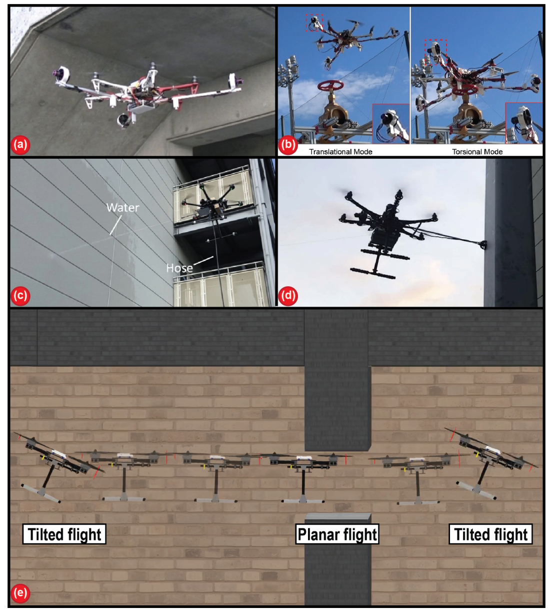

Fig. 1. (a). Add-on Translation Driving system (ATD). (b). Thrust vectored device used for aerial torsional work. (c). Thruster components used for high pressure washing (d). Physical contact with wall for NDT inspection with single thruster. (e) Concept of multirotor with two horizontal thrusters traversing narrow gap

I. Introduction

The maintenance of industrial and civil infrastructures has emerged as a prominent domain where Unmanned Aerial Vehicles (UAVs) demonstrate notable effectiveness [1]. Specifically, the application of UAVs in contact inspection and non-destructive inspection (NDT) has garnered significant interest [2], [3], [4], [5], [6]. In these applications UAVs are employed to assess the condition of infrastructure across diverse industries, showcasing their versatility in inspection tasks. In general, two distinct categories of vehicles emerge based on the characteristics of their propellers and, consequently, their method of actuation. The prevalent type is represented by under-actuated vehicles [2], [3], [4], which dominate the commercial landscape. To apply the necessary contact forces for inspection, these vehicles tilt towards the object of interest, effectively directing the resultant thrust vector. From a construction standpoint, under-actuated vehicles are known for their simplicity, making them easy to build and customize. Additionally, their control systems are extensively researched, often allowing for the implementation of straightforward controllers tailored to the specific task at hand. However, this approach greatly limits the forces that can be exerted, and place the vehicle in a constrained state. The coupled relationship between the vehicle's moment and force limit the available control options. Fully-actuated vehicles are characterized by the placement or control of propellers at non-collinear orientations, enabling the separation of attitude and forces to suit the demands of inspection and manipulation tasks [5], [6], [7]. The research described in [5] presents a fully-actuated vehicle equipped with tilting propellers, enabling the vehicle to interact with curved surfaces. This concept is further developed in [6], where the system manipulator is equipped with a rolling sensor. This sensor enables the vehicle to assess the corrosion condition of reinforced concrete as it moves along the surface of the structure. In [7], a vehicle featuring six coplanar-center propellers in a tilted configuration is equipped with an eddy current (EC) sensor for pipe inspection tasks. These systems offer greater degrees of motion and further increase the forces available for manipulation. However, it's worth noting that their implementation often necessitate a larger number of actuators, and their controllers tend to be more intricate compared to under-actuated counterparts. Consequently, this complexity renders them less accessible, with their deployment predominantly confined to the research

Department of Robotics, Graduate School of Science and Engineering, Ritsumeikan University, Kusatsu 525-8577, Japan gr0396fe@ed.ritsumei.ac.jp

sector, despite some industrial implementations existing.

Our proposal aims to find a balance between the simplicity of under-actuated vehicles and the advanced control capabilities of fully-actuated counterparts. While certain application requirements may surpass the capabilities of commercial UAVs, such constraints don't necessitate all the control options of fully-actuated systems. To enhance the manipulation and movement capabilities of conventional multirotors, our approach involves strategically incorporating additional thrust components based on the specific manipulation task at hand. The nature of the forces and torques required for manipulation is determined by the task. This consideration influences decisions about the design of the system, including determining the appropriate number of actuators, their positions, and orientations. Figure 1 illustrates various applications utilizing add-on thrusters, as evaluated in our previous research. In Fig. 1.a, as described in [8], the depicted approach features three electric ducted fans (EDFs) that enable both translational movements and lateral forces. Figure 1.b, as explored in [9], thrust vectoring components were incorporated, allowing the UAV to generate high torsional moments, proving effective for manipulating an industrial-grade valve. In Fig 1.c, following the approach detailed in [10], a UAV was developed for high-pressure washing tasks. The additional thrusters facilitated planar motions and effectively countered reaction forces during the washing process. Figure 1.d, features a vehicle equipped with a single thruster [11], used to evaluate physical contact with a wall. The proposed control framework facilitates the seamless integration and control of additional thrusters, enabling autonomous control for different actuator configurations. Furthermore, it allows the vehicle to switch flight modes mid-flight, exemplified in Fig. 1.e. Here, a multirotor with two horizontal thrusters demonstrates the capability to transition between normal tilted flight and planar flight, allowing it to cross narrow gaps with ease. For these vehicles, we modified the under-actuated multirotor controller embedded in the PX4 Autopilot firmware. Our modification extends its capabilities to support different types of flight, encompassing both limited planar and fully-planar flight modes. The main contributions of this paper are summarized as follows:

- The development of control strategies which allows for integration of horizontal thrusters and the support for directional thrust and planar flight.
- The design and simulation of multirotors with different thruster configurations, exploring different setups to assess performance and maneuverability
- A comparative analysis between simulated results and the practical implementation of the proposed system in real hardware.

II. Multirotors with additional horizontal thrusters

Our approach addresses the inherent requirement for precise and controlled directed forces present in many NDT tasks, as is the case with ultrasound inspections [2] and impact based inspections like hammering checks [3]. Achieving this requires control over both the multirotor's propellers and the additional thrusters dedicated to facilitating planar motions. Based on this consideration we can approach this problem as following:

- Decentralized Vectored Systems
- Integrated Vectored Systems

Decentralized Vectored Systems refer to the scenario where the control of the additional thruster is independent from that of the flight controllers. The aerial system is kept in its hover state and the additional thrusters are controlled by an on-board PC. This approach has been evaluated in our research in [8], [9], [10], [11]. Separating the control logic between thrusters and multirotor propellers, simplifies the overall control of the system, while simultaneously expanding the range of available flight and manipulation options for UAVs. However, this also means that the available actuators in the system are not able to be fully utilize. Moreover, from the perspective of the flight controller this additional actuators, represent external disturbances, which may lead to unpredictable behaviours.

Integrated Vectored Systems in contrast with the decentralized approach, have control of all the actuators present in the vehicle. Under-actuated [12] and fully-actuated [6], [5] vehicles can be controlled through an on-board PC which interfaces with their flight management unit (FMU). The main control logic and the control allocation of the system is managed by the on-board PC. Based on the desired motions and force requirements, it calculates the required thrust and attitude setpoints and send this commands to the FMU. The role of the FMU is now reserved as a communication bridge between the on-board PC, its internal sensors e.g. IMU, barometer, compass and the actuators which generate the thrust. Integrating the control logic of custom vehicles into FMU not only simplifies setup time but also makes these systems more accessible for potential users, particularly those with limited experience. This in turn frees the on-board PC to be used for other processing tasks, such as state estimation, control of manipulators and image processing. Moreover, in the event of communication interruptions with the on-board PC, the flight controller retains control of the actuators responsible for flight. Conversely, for less complex tasks involving semi-autonomous or manual operations, external sensors connected to flight controller such as GPS modules, optical flow cameras, or distance sensors, are sufficient.

A. Proposed control strategies for thrusters

For the purpose of our applications we selected the PX4-Autopilot [13], which is an open source firmware often used for research and commercial vehicles. Out of the box the flight controller offers supports for different types of vehicles, such as multirotors, fixed wings vehicles, ground and underwater vehicles. The type of vehicle selected determines control strategies of the vehicle and the manner in which the actuators will be commanded. Previous research, as detailed in [14], have successfully implemented strategies to enhance version V1.10.1 of the PX4 firmware, facilitating the control of fully-actuated vehicles. This research also

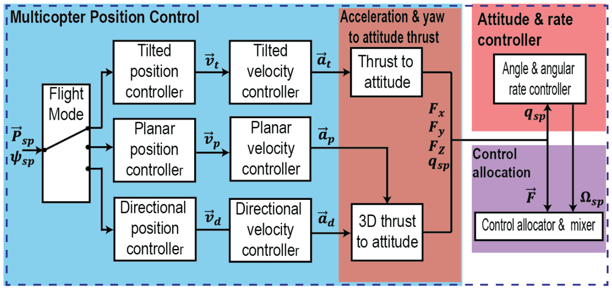

Fig. 2. Multicopter Position Controller diagram software modifications

provided valuable insights into the inner workings of the PX4 firmware at that time. Our research extends and builds upon the current version, v1.14.0, by introducing support for multirotors equipped with additional thrusters or propellers positioned at non-collinear orientations. A diagram illustrating the modified control blocks in the PX4 architecture is presented in Fig. 2. In recent firmware versions, the **Control allocation** block has been incorporated as the default method for governing the actuators of the vehicle. As implied by its name, the control allocation matrix is generated based on the position and orientation of all actuators within the system. The geometric arrangement of the propellers and additional actuators, determine the control capabilities of the UAV. Although, the firmware allows for the customization of each actuator's position and orientation, the control of these actuators and in turn the type of flight is bounded by the vehicle type selected. All the vehicles which are classified as multirotors will have the same control behavior, regardless of the orientation of the additional propellers. The vehicle will control its angular rates to orient its thrust vectors to fulfill the commanded setpoints. The frame convention adopted was North-East-Down (NED) when referencing the inertial frame $\mathcal{F}_I$, and Forward-Right-Down (FRD) for the body frame $\mathcal{F}_B$. In addition $\hat{x}_B$, $\hat{y}_B$, and $\hat{z}_B$ refer to unit vectors aligned with the axes of the body frame. In a general sense, the **Multicopter position control** block computes the necessary thrust and attitude commands based on a provided set of initial position $\vec{P_{sp}}$ and yaw $\psi_s p$ setpoints. Where $\vec{P_{sp}}$ denotes either the operator's transmitter commands, internal predefined trajectories, or trajectories specified by an onboard PC. How the thrust and the attitude is computed, depends on the selected flight mode. The current system supports three primary flight modes: a **tilted flight mode**, a **planar flight mode**, and a **directional thrust flight mode**.

In **tilted mode**, the vehicle adheres to the default PX4 multicopter controller, having full command of its roll and pitch axes. Maintaining the system in flight, is given priority in all the calculations of the system. Within the velocity controller, the computation of (a_{tx}, a_{ty}) components is intricately tied to the vertical acceleration a_{tz}. These horizontal components are coupled, and are calculated based on the remaining thrust capabilities of the vehicle once the vertical component a_{tz} has been satisfied. In the **Thrust to attitude** block, the initial step involves deriving a preliminary force vector $\vec{F}$ from the solved acceleration vector $\vec{a}_t$. This force vector is then utilized to calculate the unit vectors $\hat{x}_B$, $\hat{y}_B$, and $\hat{z}_B$. These unit vectors, in turn, define the desired orientation quaternion q_{sp}. Is important to note that the direction of $\vec{F}$ is opposite to $\hat{z}_B$. Therefore, we can express the following:

$$\hat{z}_B = \frac{-\vec{F}}{\|\vec{F}\|} \tag{1}$$

$$\hat{y}_c = \begin{bmatrix} -sin\psi_{sp} & \cos\psi_{sp} & 0 \end{bmatrix}^T \tag{2}$$

Where y_c refers to a vector in the direction of ψ_{sp} in the xy-plane, rotated $\pi/2$ around the the z-axis of the inertial frame $\mathcal{F}_I$.

$$\hat{x}_B = \hat{y}_c \times \hat{z}_B \tag{3}$$

$$\hat{y}_B = \hat{z}_B \times \hat{x}_B \tag{4}$$

The obtained attitude from the unit vectors in (1), (3), (4) is later constrained by the maximum allowable tilt of the vehicle. Following this, the system generates a thrust vector with a vertical force component F_z and an orientation q_{sp}. This corresponds to the standard thrust and orientation calculation commonly employed by multirotors.

On the other hand, the **planar mode** facilitates lateral motions while maintaining roll and pitch angles close to zero degrees. This mode is specifically designed for configuration with actuators capable of directly generating forces along the x and y axes of the vehicle. In contrast to the previously mentioned tilted mode, the vertical component of acceleration of a_{pz} is decoupled from the planar components (a_{px}, a_{py}). The desired altitude setpoint can be now satisfied without constraining lateral accelerations. Furthermore, planar vehicles necessitate the computation of individual force components (F_x, F_y, F_z), alongside a zero roll and pitch attitude setpoint q_{sp}. In the case of a zero tilt attitude, the unit vector z_B is aligned downward, parallel to the z-axis of the reference frame $\mathcal{F}_I$, shown as:

$$\hat{z_B} = \begin{bmatrix} 0 & 0 & 1 \end{bmatrix}^T \tag{5}$$

The remaining unit vectors $\hat{x}_B$ and $\hat{y}_B$, will be rotated in the xy-plane by the yaw angle setpoint ψ_{sp}, as shown below:

$$R_I = \begin{bmatrix} \cos(\psi_{sp}) & -\sin(\psi_{sp}) & 0 \\ \sin(\psi_{sp}) & \cos(\psi_{sp}) & 0 \\ 0 & 0 & 1 \end{bmatrix} \tag{6}$$

The desired force components (F_x, F_y, F_z) are then computed using their corresponding acceleration components (a_{px}, a_{py}, a_{pz}). Subsequently, the constructed vector $\vec{F}$ is forwarded to the control allocator, tasked with distributing the desired forces among the vertical rotors and the horizontal thrusters.

The **directional thrust mode** combines control strategies from both tilted and planar flight modes, permitting planar flight along certain axis while controlling its roll or pitch angles, for the remaining motions. Directional thrust flight is achieved by computing the force components (F_x, F_y, F_z), and the tilted and planar components of the attitude q_{sp}.

When actuators are unable to provide a planar motion in a certain direction, the system will follow the tilted mode force and attitude calculation. The attitude is calculated similar to the tilted mode, where the unit vector $\hat{z}_B$ depends on the force vector $\vec{F}$. However, this force vector, is first evaluated with respect to the body frame $\mathcal{F}_B$, by rotating it using the yaw setpoint ψ_{sp}, as illustrated below:

$$R_B = \begin{bmatrix} \cos(-\psi_{sp}) & -\sin(-\psi_{sp}) & 0 \\ \sin(-\psi_{sp}) & \cos(-\psi_{sp}) & 0 \\ 0 & 0 & 1 \end{bmatrix} \tag{7}$$

$$\vec{F}_B = R_B \times \vec{F} \tag{8}$$

The procedure involves modifying the vector $\vec{F}_B$ to accommodate both tilted and planar motions effectively. Depending on the configuration of the actuators, planar forces can be generated in specific directions along the horizontal axes. To handle this, the horizontal force components corresponding to the desired planar motion are isolated from $\vec{F}_B$ and stored separately in a vector denoted as $\vec{F}_p$. Subsequently, the remaining vertical and horizontal components are used to construct the force vector representing the tilted motions, referred to as $\vec{F}d$.

Similar to the thrust and orientation calculations discussed in the tilted mode, F_d is utilized to compute $\hat{z}_B$. For instance, when aiming for planar motion along the x-axis of the body frame, the x-force component is nullified (set to 0).

$$\hat{z}_B = \frac{-\vec{F}_d}{\|\vec{F}_d\|} \tag{9}$$

To achieve planar motions along the x-axis, it is necessary to set the pitch angle to 0. Consequently, the definition of $\hat{x}_B$ becomes:

$$\hat{x_B} = \begin{bmatrix} \cos\psi_{sp} & \sin\psi_{sp} & 0 \end{bmatrix} \tag{10}$$

And $\hat{y}_B$ will remain same as (4).

Likewise for planar motions along the the y-axis, the roll angle will be set to 0. Therefore, $\hat{x}_B$ and $\hat{y}_B$ will be defined as:

$$\hat{x_B} = \hat{y_B} \times \hat{z_B} \tag{11}$$

$$\hat{y_B} = \begin{bmatrix} -\sin\psi_{sp} & \cos\psi_{sp} & 0 \end{bmatrix} \tag{12}$$

The attitude, as represented by the unit vectors, is subsequently constrained by the maximum permissible tilt, establishing the attitude setpoint q_{sp}. The desired force components (F_x, F_y, F_z) are composed of the vertical component of $\vec{F}_d$ and the horizontal components of $\vec{F}_p$. These new vector F is then sent to the control allocator, which distributes the desired forces in the vertical rotors and the horizontal thrusters.

The available modes for a UAV depend on the number and configuration of its actuators. Vehicles capable of generating planar forces along both the x and y axes can employ all three control strategies. On the other hand, UAVs with a more constrained actuator configuration, producing forces in limited directions, are designed to transition specifically between tilted mode and directional thrust mode.

III. SIMULATIONS

The control strategies described earlier were assessed in the Gazebo simulation environment, using the Software-In-The-Loop (SITL) capabilities of the PX4 firmware. Fig. 3 illustrates the various vehicles designed for evaluation. The additional thrusters, depicted in red, are positioned horizontally in relation to the main propellers of the multirotors. Each configuration underwent testing within a rectangular trajectory, measuring 0.8 m in width and 1.2 m in length, illustrated in Fig. 4. The trajectory starts at the bottom-left corner of the rectangle, with the vehicle moving anti-clockwise through successive points and transitioning between available modes. The elements in each set of coordinates represent the x, y, z positions in meters, and the last element corresponds to the yaw angle in degrees.

A. Single Thruster Configuration

This vehicle type corresponds to multirotors equipped with an additional thruster capable of generating thrust in the xy-plane. These vehicles utilize control strategies from the tilted mode and directional thrust mode. The configuration depicted in Fig. 3.a showcases a quadrotor equipped with an additional thruster aligned along its x-axis. This configuration allows the vehicle to execute planar motions exclusively when moving forward. To navigate backward, towards the negative direction of the x-axis, the system adjusts its pitch angle ϕ. Similarly, lateral motions are accomplished by changing its roll angle θ. Fig. 5 represents the attitude change when the system traverses a rectangular trajectory. The vertical dotted lines denote the trajectory's starting point on the the bottom-left corner of the rectangle shown in Fig. 4. During the **normal flight mode**, the multirotor follows the tilted mode control strategy. In the **single planar thrust** section of the plot, the pitch angle in the negative orientation, has been reduced, and the thruster is now used for the forward motion. The system maintains full control over its roll angle and retains the capability to adjust the negative pitch angle as needed.

B. Dual Thruster Configuration

The vehicle in Fig. 3.b depict a quadrotor with two thruster positioned along its x -axis but oriented in opposite

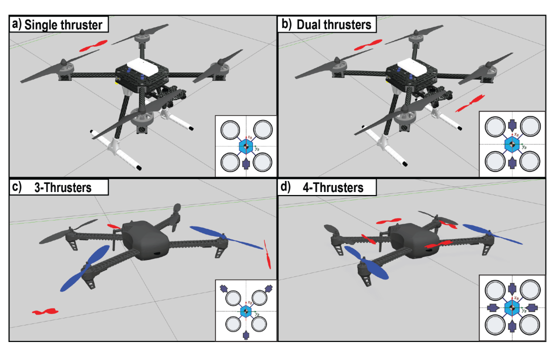

Fig. 3. Simulation of different thruster configuration on multirotors. The horizontal thrusters are depicted by red propellers

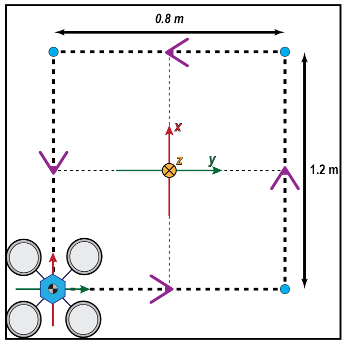

Fig. 4. Rectangular trajectory for autonomous flight experiment

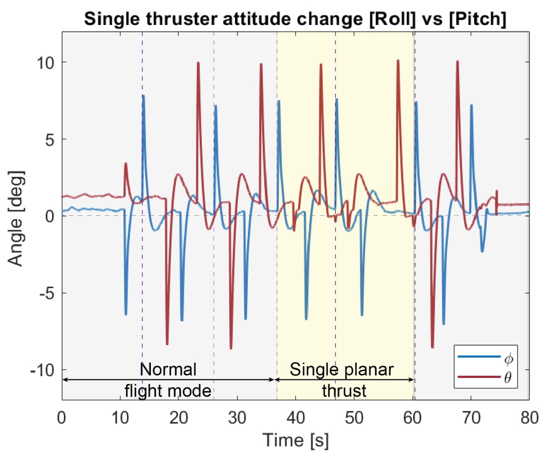

Fig. 5. Evaluation of single thruster configuration in rectangular trajectory

directions. The addition of these actuators allow the system to use the directional thrust strategy along its x-axis. Figure 5, demonstrates the transition from the **normal flight mode** to the **dual thrust planar mode**, where the pitch angle is maintained close to zero degrees, during the planar motion. The system maintains full control over its roll and utilizes the thruster for moving in both directions of the x-axis. Furthermore, this configuration retains the flight modes present in the single thruster variation, as shown in the **single planar thrust** section of the plot.

C. 3-Thrusters Configuration

The configuration shown in Fig. 3.c represents minimum number of thrusters required for planar movement in the xy-plane. Three EDFs are positioned at a separation of 120° from from each other. This particular configuration has been previously explored in our research on [10], [9]. During forward movement along the x-axis, a single thruster is employed, while backward motions utilize the remaining two thrusters. For lateral movement along the y-axis, a pair of thrusters is always required. In addition of employing the control strategies for planar flight, planar vehicles are capable of transitioning to directional thrust mode for limited planar motions or tilted mode for normal flight. This is demonstrated in Fig. 7, where the vehicle changes between the 3 control strategies present in the controller. The **full planar thrust** section of the plot illustrate the change of the roll and pitch angles, when compared to the other sections. Though the system is capable of transitioning between three proposed modes, it exhibits less precision for smaller motions when compared to the other vehicles. This is evident after the transition to full planar thrust, as the vehicle resumes movement along the trajectory until the 60th second. This delay arises from the vehicle not converging near the initial setpoint after the mode change.

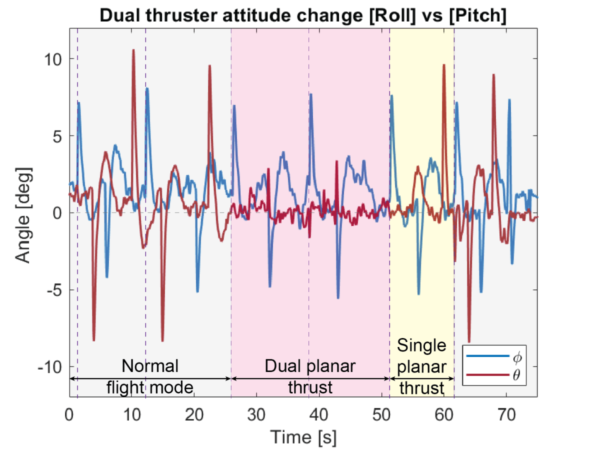

Fig. 6. Evaluation of dual thrusters configuration in rectangular trajectory

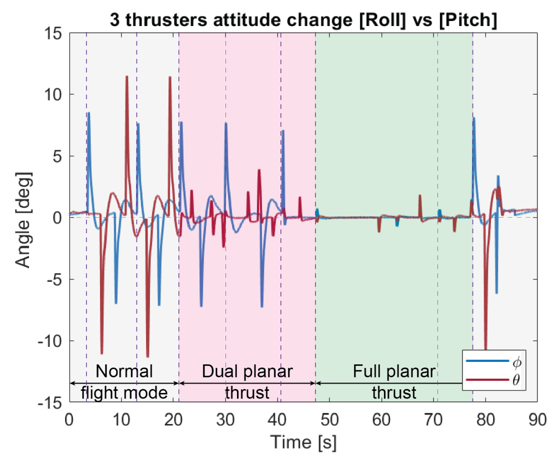

Fig. 7. Evaluation of the 3-thrusters configuration in rectangular trajectory

D. 4-Thruster Configuration

Similar to the 3-thrusters variation, the configuration illustrated in Fig. 3.d enables planar motion. This configuration provides an enhanced level of control compared to previous setups. Dedicated actuators are integrated into the system for motion along both the positive and negative directions of the x and y axes. Furthermore, the independence of actuators and axes facilitates a more precise control of the thrust vector. This flexibility enables support for all the developed control strategies and includes the subset of motions present in the other thruster configurations. Figure. 8 illustrates the attitude change during the transition between the available flight

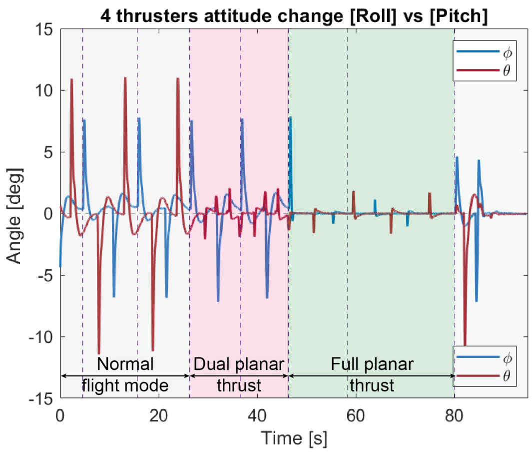

Fig. 8. Evaluation of the 4-thrusters configuration in rectangular trajectory

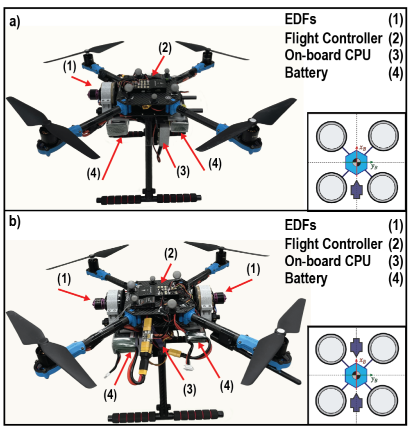

Fig. 9. Developed prototypes for single and dual thrusters configuration

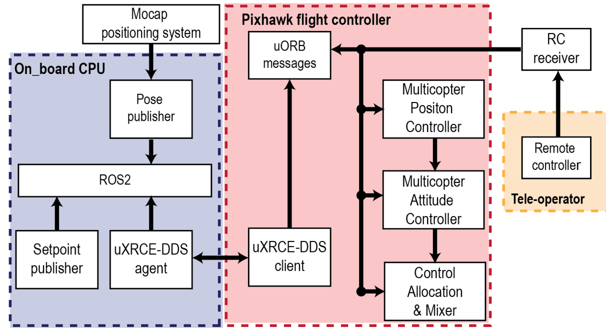

Fig. 10. Block diagram illustrating the communication flow within the developed system

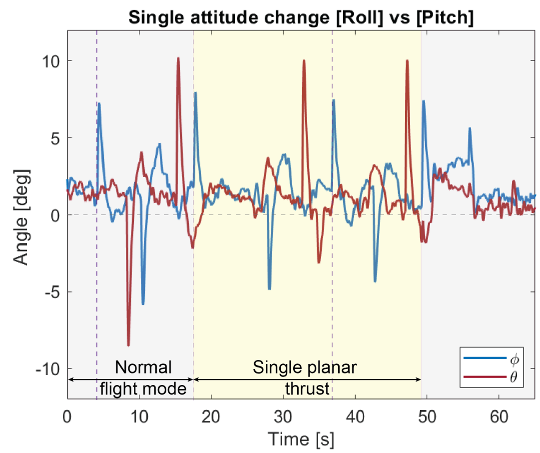

Fig. 11. Practical evaluation of single thruster configuration in rectangular trajectory

modes. Moreover, the delay present in the 3-thruster vehicle after the transition to full planar thrust mode, is absent in this configuration. Nevertheless, both configurations display similar planar behavior once the trajectory commences, and their orientations are maintained close to zero degrees.

IV. Hardware Evaluation

To validate the simulation results, the proposed control framework was assessed on real hardware. The tested configurations, as depicted in Fig. 9, encompass both the single thruster and the dual thruster configuration. The test vehicle is built upon a Holybro X500 v2 quadcopter airframe, enhanced with a set of EDFs, to serve as supplementary thrusters. The vehicle and its actuators are controlled by a Pixhawk 6C flight controller, operating on our proposed thrust control firmware. Through the open-source ground control station (GCS) software, information regarding the position and orientation of the additional thrusters can be configured. In addition, custom planar parameters have been created to tune the vehicles planar controllers, limit the horizontal velocities and select the modes to be evaluated. The control strategies of the different flight modes and support for additional actuators is included within the programming of the custom firmware in the flight controller's PC. As illustrated by Fig. 10, an Intel UP board 4000, running Ubuntu 22.04 with a ROS2 Humble distribution, acts as the on-board PC. Utilizing uXRCE-DDS for agent and client communication, it actively monitors and provides positioning and navigation data to the flight controller. This positioning data is obtained from a motion capture system which communicates with the on-board PC through the ROS2 environment. This off-board information is used by the UAV, enabling tasks such as maintaining position and following setpoints. Similar to the simulation scenario, the vehicles were evaluated in a rectangular trajectory, illustrated in Fig. 4 . Based on the actuators configuration, the vehicles will transition between the available modes while traversing through the waypoints.

A. Flight Experiments: Single Thruster

The evaluated single thruster system is shown in Fig. 9.a, where an EDF is attached along its x-axis. Figure. 11, illustrates the system's attitude during the flight mode transition. Furthermore, Fig. 12 shows the phase of the flight experiment during which the vehicle transitions to the single planar thrust mode. The results exhibit a consistent behavior with the corresponding simulated case, showcasing the utilization of thrusters for necessary forward motions in the trajectory. Additionally, the vehicle employs the control of its roll θ and

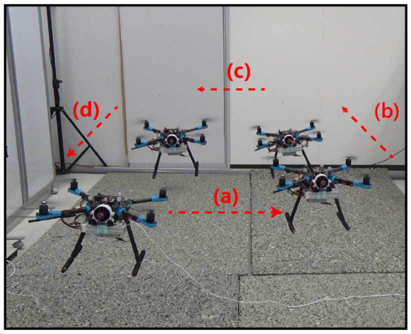

Fig. 12. Flight sequence during single planar thrust. (a) Positive roll angle θ (b) Forward planar motion (c) Negative roll angle orientation θ (d) Positive pitch angle ϕ

pitch ϕ for the remaining motions.

B. Flight Experiments: Dual Thruster

The evaluated dual thruster system is depicted in Fig. 9.b, where 2 EDFs are attached opposite to each other, along the frame's x-axis. Fig. 14, illustrates the system's attitude during the flight mode transition. The segment of the flight experiment demonstrating the dual planar thrust mode is depicted in Fig. 13. Likewise the results remain consistent with the corresponding simulated case, across all three sections of the experiment. Full control over the vehicle's roll angle is maintained, and the two EDFs enable bidirectional planar motion along the x-axis. Additionally, as observed in simulations, this configuration retains the flight modes present in the single thruster variation.

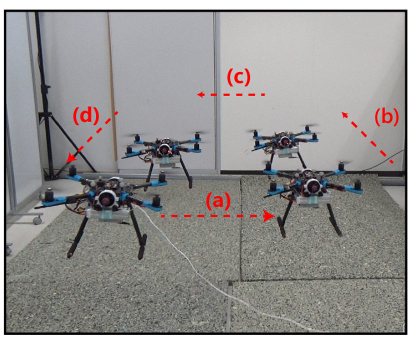

Fig. 13. Flight sequence during dual planar thrust. (a) Positive roll angle θ (b) Forward planar motion (c) Negative roll angle orientation θ (d) Backward planar motion

V. CONCLUSIONS

In this research, we introduce a control and design framework to enhanced the manipulation capabilities of under-actuated multirotors. This approach aims to improve the capabilities of under-actuated vehicles, avoiding the additional complexities associated with fully-actuated counterparts. This control framework enables the implementation of various flight types, adapting to the available actuators in the vehicle. The customizable nature of this approach allows for tailoring the system to specific tasks, accommodating scenarios where either directional thrust or full planar forces

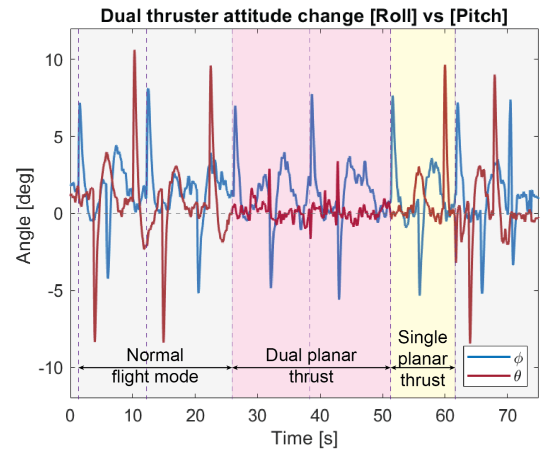

Fig. 14. Practical evaluation of dual thrusters configuration in rectangular trajectory

prove sufficient. Moreover, the ability to transition to the normal flight mode, allows the thrusters be used only when these needed. The control strategies and logic to support the enhance actuation of this approach, have been embedded in the flight controller. We have evaluated our system through simulations, where vehicles with different actuator configurations have been tested. These simulations were validated in real world experiments, with a UAV with equipped thrusters and a flight controller running our modified firmware.

Future iterations of this work will further develop and assess the concept depicted in Fig. 1. While certain under-actuated vehicles might navigate the gap with dynamic maneuvers and forward momentum, the ongoing research offers a potentially safer alternative for obstacle traversal. However, within elongated corridors or tunnels, as illustrated in Fig. 15, even if the vehicle successfully enters, due to the space it loses the ability to tilt. Moreover, sustaining flight inside the corridor necessitates the vehicle to grapple with the aerodynamic effects from both the ceiling and the walls [15]. We will thoroughly evaluate the efficacy of our strategies under these challenging conditions.

Moreover, we will investigate the integration of tiltable thrusters into under-actuated vehicles. This integration enables control over the thrust vector, thereby enhancing movement capabilities and expanding the range of forces that the multirotor can generate.

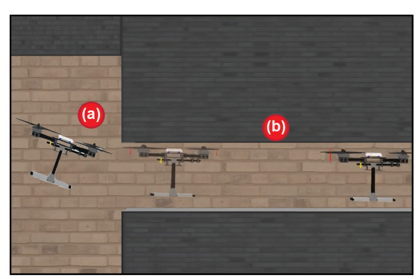

Fig. 15. Flight through narrow corridor. (a). Tilted flight (b). Planar flight

ACKNOWLEDGMENT

This work was partially supported by JST, CREST Grant Number JPMJCR22C1, Japan.

REFERENCES

[1] P. Nooralishahi, C. Ibarra-Castanedo, S. Deane, F. López, S. Pant, M. Genest, N. P. Avdelidis, and X. P. V. Maldague, "Drone-based non-destructive inspection of industrial sites: A review and case studies," *Drones*, vol. 5, no. 4, 2021. [Online]. Available: https://www.mdpi.com/2504-446X/5/4/106

[2] D. Zhang, R. Watson, C. MacLeod, G. Dobie, W. Galbraith, and G. Pierce, "Implementation and evaluation of an autonomous airborne ultrasound inspection system," *Nondestructive Testing and Evaluation*, vol. 37, no. 1, pp. 1–21, 2022.

[3] T. Ikeda, S. Yasui, S. Minamiyama, K. Ohara, S. Ashizawa, A. Ichikawa, A. Okino, T. Oomichi, and T. Fukuda, "Stable impact and contact force control by uav for inspection of floor slab of bridge," *Advanced Robotics*, vol. 32, no. 19, pp. 1061–1076, 2018.

[4] L. González-deSantos, J. Martínez-Sánchez, H. González-Jorge, F. Navarro-Medina, and P. Arias, "Uav payload with collision mitigation for contact inspection," *Automation in Construction*, vol. 115, p. 103200, 2020. [Online]. Available: https://www.sciencedirect.com/science/article/pii/S0926580519314207

[5] K. Bodie, M. Brunner, M. Pantic, S. Walser, P. Pfändler, U. Angst, R. Siegwart, and J. I. Nieto, "An omnidirectional aerial manipulation platform for contact-based inspection," *CoRR*, vol. abs/1905.03502, 2019.

[6] P. Pfändler, K. Bodie, G. Crotta, M. Pantic, R. Siegwart, and U. Angst, "Non-destructive corrosion inspection of reinforced concrete structures using an autonomous flying robot," *Automation in Construction*, vol. 158, p. 105241, 2024. [Online]. Available: https://www.sciencedirect.com/science/article/pii/S0926580523005010

[7] M. Tognon, H. A. T. Chávez, E. Gasparin, Q. Sablé, D. Bicego, A. Mallet, M. Lany, G. Santi, B. Revaz, J. Cortés, and A. Franchi, "A truly-redundant aerial manipulator system with application to push-and-slide inspection in industrial plants," *IEEE Robotics and Automation Letters*, vol. 4, no. 2, pp. 1846–1851, 2019.

[8] R. Miyazaki, H. Paul, and K. Shimonomura, "Development of add-on planar translational driving system for aerial manipulation with multirotor platform," *Applied Sciences*, vol. 11, no. 4, 2021. [Online]. Available: https://www.mdpi.com/2076-3417/11/4/1462

[9] R. R. Martinez, H. Paul, and K. Shimonomura, "Aerial torsional work utilizing a multirotor uav with add-on thrust vectoring device," *Drones*, vol. 7, no. 9, p. 551, 2023.

[10] R. Miyazaki, H. Paul, T. Kominami, R. R. Martinez, and K. Shimonomura, "Flying washer: Development of high-pressure washing aerial robot employing multirotor platform with add-on thrusters," *Drones*, vol. 6, no. 10, 2022. [Online]. Available: https://www.mdpi.com/2504-446X/6/10/286

[11] T. Kominami, Z. Liang, R. R. Martinez, H. Paul, and K. Shimonomura, "Physical contact with wall using a multirotor uav equipped with add-on thruster for inspection work," in *2023 IEEE/RSJ International Conference on Intelligent Robots and Systems (IROS)*. IEEE, 2023, pp. 6955–6961.

[12] T. Baca, M. Petrlik, M. Vrba, V. Spurny, R. Penicka, D. Hert, and M. Saska, "The mrs uav system: Pushing the frontiers of reproducible research, real-world deployment, and education with autonomous unmanned aerial vehicles," *Journal of Intelligent & Robotic Systems*, vol. 102, no. 1, p. 26, 2021.

[13] L. Meier, D. Honegger, and M. Pollefeys, "Px4: A node-based multithreaded open source robotics framework for deeply embedded platforms," in *2015 IEEE International Conference on Robotics and Automation (ICRA)*, 2015, pp. 6235–6240.

[14] A. Keipour, M. Mousaei, A. Ashley, and S. Scherer, "Integration of fully-actuated multirotors into real-world applications," pp. 1–8, in press.

[15] A. Ollero and B. Siciliano, Eds., *Aerial Robotic Manipulation - Research, Development and Applications*, ser. Springer Tracts in Advanced Robotics. Springer, 2019, vol. 129. [Online]. Available: https://doi.org/10.1007/978-3-030-12945-3